

**NASA Technical Memorandum 85689**

NASA-TM-85689 19840008359

**SURFACE ACCURACY MEASUREMENT SENSOR TEST  
ON A 50 METER ANTENNA SURFACE MODEL**

**R.B. SPIERS, E.E. BURCHER, C.W. STUMP,  
C.G. SAUNDERS, AND G.F. BROOKS**

**JANUARY 1984**

**FOR REFERENCE**

**NOT TO BE TAKEN FROM THIS ROOM**

**LIBRARY COPY**

**FEB 2 1984**

**LANGLEY RESEARCH CENTER  
LIBRARY, NASA  
HAMPTON, VIRGINIA**



**National Aeronautics and  
Space Administration**

**Langley Research Center  
Hampton, Virginia 23665**



## SUMMARY

Future large space structures in Earth orbit will require an alignment measuring system to verify the structural design conformance in a space environment. A Surface Accuracy Measurement Sensor (SAMS) engineering breadboard was laboratory tested and then field tested on a 30 degree portion of a 50 meter diameter surface antenna model. The sensor tests, using both light emitting diodes and retro directive targets, proved successful and, consequently, should be a strong candidate for space use as a real time measurement device. Test results are presented with recommendations for sensor improvements.

#  
A84-16427

## INTRODUCTION

The deployment of or fabrication of Large Space Structures (LSS) in Earth orbit will require structural alignment sensors to measure and verify the structural conformance with the design. Such alignment sensors are similar to the surveyor's transit or theodolites used on Earth to measure construction tolerances. The fabrication tolerances of some LSS require precisions beyond that of typical Earth construction and, furthermore, must be measured remotely in the environment of orbital space. For example, a 100 meter diameter, 15 gigahertz, microwave, mesh antenna, requires a surface accuracy measurement capability of better than  $\frac{\lambda}{100}$ , which is 0.20 millimeters (mm) (0.008 inch), RMS. A sensor to make these measurements must be light in weight and small in size to minimize the interference with either the very lightweight construction or the antenna operation. NASA Langley Research Center (LaRC) through two contracts (references 1 and 2) with TRW Defence and Space Systems Group, Redondo Beach, California, has developed an engineering breadboard model of a Surface Accuracy Measurement Sensor (SAMS) for the Large Space Structures Technology (LSST) program. The breadboard sensor was delivered to LaRC where it was electronically modified, tested, and calibrated. The sensor was transported to the Harris Corporation in Florida and tested on their 50 meter diameter Hoop/Column Mesh Antenna Model to determine its measurement stability and accuracy when compared with a Harris Corporation theodolite triangulation measurement system.

### Sensor Description

The SAMS is a telescope with a focal plane photoelectric detector which senses the position of several small light source targets in its field of view. Target distances are typically 5 to 50 meters. It does not sense target distance along the telescope's optical axis; rather, it senses the angular displacements relative to the electro-optical axis. If the target distances from the telescope entrance aperture is known, target deflections normal to the electro-optical axis can be calculated. A typical angular sensitivity is 0.5 arc secs. at a target distance of 20 meters which gives a target deflection of 60 micrometers. The sensor consists of (1) an anamorphic telescope receiver, (2) several light emitting diode (LED) targets, (3) an LED modulatable power supply, (4) signal processing electronics and (5) a computer for data processing.

Telescope receiver.- The receiver is an anamorphic telescope shown in figure 1. Target radiation entering the telescope objective lens is imaged on a linear effect planar silicon photodiode which has a sensitive area 5 mm long and 2 mm wide. The detector is oriented so its long dimension is along the direction of the target deflection to be measured, the y-axis. The axis of a cylindrical field lens is also oriented in the direction of the target deflection to be measured. The lens is positioned along the telescope optical axis so its focal power in the x-z plane forms an image of the telescope objective on the detector. The image size is about 1 mm. It can be demonstrated that a target motion in the x-y plane will cause the image on the detector to move only in the y direction. The image will move a distance proportional to the distance of the y component of the target motion. The anamorphic telescope described is a single axis measurement receiver. A beam splitter placed just before the cylindrical lens and the addition of another cylindrical lens and

detector oriented along the x-axis will give a 2 axis measurement receiver. The present breadboard sensor shown in figure 2, is a single axis receiver.

The linear effect photodiode gives two signal outputs,  $I_A$  and  $I_B$ , one from each end of the detector. The amplitudes of these two signals are proportional to the image intensity on the detector and on the relative position of the image along the length of the detector. That is, the image motion along the detector, which is proportional to the target motion, causes the signals for the two ends of the detector to increase and decrease, respectively. This later effect gives the detector its linear measurement capability. The former effect which may be caused by a change in the intensity of the target sources will also cause the signals to increase and decrease and confuse any linear measurement capability. A unique solution to this problem is available using the following technique.

The intensity of the LED targets is modulated with a square wave generator causing the signals from the detector to also have a square waveform. These signals are amplified, digitized, multiplexed and fed into a computer for data processing, see figure 3. The amplitudes of these signals  $I_A$  and  $I_B$ , are measured and applied to the algorithm:

$$Y = \frac{L_D}{2} \frac{(I_A - I_B)}{(I_A + I_B)}$$

$Y$  = Detector image displacement ( $\pm$  about the electro-optical axis)

$L_D$  = Detector sensitive length

This algorithm gives a numerical value that is insensitive to any amplitude changes which are common to both signals. That is, detector signal amplitude changes produced by the light levels of different targets, image intensity changes produced by atmospheric scintillations, electrical signal changes to the detector that are common to both signal outputs. Only changes in signals

due to image motion along the detector are sensed. The computer samples the data output of the detector and plots the solution to the algorithm versus actual target displacement,  $\Delta$ , to give a calibration of the sensor, see figure 4. The equation used to calculate target displacement is given by:

$$\Delta = \frac{YD}{d}$$

where  $d$  is the telescope focal length and

$D$  is the target distance.

The maximum angular displacement is given by:

$$\pm \theta = \frac{\pm Y}{d}$$

Note that as  $I_A$  approaches zero,  $I_B$  approaches a maximum value and the algorithm value approaches 1. Figure 4 shows the sensor does not have a linear response over the entire range of measurement angles. Therefore, to obtain the best accuracy with this sensor it must be used over a very linear portion of the curve near the electro-optical axis or the sensor must be calibrated with standard target displacements.

LED targets.— The LED targets are P-N Gallium Arsenide infrared emitting diodes which emit 0.9 micrometer radiation in a hemispherical pattern. The diode has a hemispherical lens about 72 mils in diameter and has a total radiant power output of approximately 123 milliwatts per ampere of input current. Its maximum current is 3 amperes. Because this diode radiates in the wavelength band of the detector's maximum spectral sensitivity, the SAMS makes very efficient use of the available target power, requiring relatively small LED currents. The targets have two basic requirements. They must provide sufficient radiant power to the telescope receiver to give a suitable signal to noise ratio. They must also emit radiation over a large enough

angular pattern to insure the radiation will always enter the telescope receiver regardless of target displacements or orientation. To give further efficiency of radiant power to the targets the hemispherically emitting pattern of the LED is more efficiently directed towards the receiver. A lens is placed in front of the LED so most of the LED radiation is collected and directed towards the receiver in an approximately  $20^\circ$  solid angular pattern. This increases the amount of radiant power on the detector and does not make the target pointing requirements too stringent. A diagram of the LED target is given in figure 5. The modulatable-power supply to direct the LED output in a square waveform at 40 hertz is shown in figure 6.

Another target being considered is a retrodirective reflector, glass corner cube, with a small angular glass wedge placed over one half its aperture to deviate the returning reflected radiation so it will be incident on the telescope receiver instead of the LED source placed beside the telescope receiver, see figures 7 and 8. This makes a passive target source which does not require electrical power leads which can interface with some very lightweight large space structure such as the hoop/column mesh microwave antenna. This type of target has been demonstrated, and works very well, but there is no way for the receiver to discriminate between a large number of targets located in a single telescope's field of view; whereas, the electric powered LEDS can be sequenced on and off to provide discrimination. Some ideas on discrimination between passive targets needs further study.

Systems electronics.— The SAMS electronics serve to: (1) select and modulate the LED target; (2) amplify and digitize detector output signals; (3) provide timing and control functions for signal processing; and (4) perform algorithm calculations for deformation results. Figure 9 is a schematic of the SAMS electrical system.



The LED drive electronics provide a modulated constant current that is selectable from 0 to 1 ampere. Modulation is from an external, 40 Hz, square wave, source.

Timing and control electronics receives a signal from a function generator that is 16 times the modulation frequency. It divides this down to provide start pulses to the 16 bit A/D, switching signals to the multiplexers, data transfer pulse to the computer, and, the 40 Hz modulation of the LED modulation. It assures that the received signals are always sampled on the same point on the square wave modulation, and that data is routed to the computer in the proper sequence.

Two dual channel pre and post amplifiers, shown in figure 10, are contained in the receiver electronics. Detector current signals are amplified and converted to voltages by the transimpedance amplifiers in the first stage of the electronics. Output voltage is given by  $e_o = I_d R_f$ ; where  $R_f = 50$  megohms and  $I_d$  = detector output current. Filtering was employed on both pre and post amplifiers, giving an overall band pass of approximately 100 Hz. Since the gain of the two postamplifiers is unity, overall transimpedance of the pre-post amplifiers is  $50 \times 10^6$  V/A.

Both receiver outputs, channel A and channel B, are simultaneously sampled and digitized by two 16 bit analog to digital (A/D) converters. These two outputs are fed to a 2 to 1 digital multiplexer where they are time shared to the computer.

The computer has two interfaces. One is the 16 bit interface through which data from the multiplexer is received and all timing and control functions are provided for LED modulation, 16 bit A/D converters, and the 2 to 1 multiplexers. The other interface, an IEEE 488, handles outputs to the

printer, plotter, and target selector. Also, during initial tests at LaRC, exact target positions, provided by a laser interferometer, were entered on this bus.

Data processing for each measurement is performed by the computer after 640 samples are taken and stored. Values for receiver channels A and B are then computed, i.e.,  $A = (A^+) - (A^-)$  and  $B = (B^+) - (B^-)$ . Then, mean values of A and B, i.e.,  $\bar{A}$  and  $\bar{B}$ , and RMS variations of A and B, are determined. The sum of  $\bar{A} + \bar{B}$  and factor C,  $C = \frac{\bar{A} - \bar{B}}{\bar{A} + \bar{B}}$ , are calculated and stored in memory. Factor C, which is dimensionless, is linearly transformed, for target displacement, to the indicated value,  $\Delta$ , by the algorithm  $\Delta = mC + b$ . Slope m is obtained by calibration tests and is dependent on both target range and detector response. Center offset, b, is zero if the initial alignment of the sensor and target is perfect. The constant m is derived by an equation of the least squares,  $m = \frac{\overline{XC} - \bar{X}\bar{C}}{S_c^2}$ , where  $S_c$  is the standard deviation of the C values and  $b = \bar{X} - m\bar{C}$ . The x values were provided by a laser interferometer used to measure target displacement during calibration at LaRC.

These values were either printed out on an 80 character line printer or plotted by an x-y plotter. They were also stored in memory for recording on digital magnetic tape.

Once data has been stored on magnetic tape, it can be recalled into memory by the computer at anytime for further formatting by various plotter/print-outs that may be desired; or for use in performing further analysis on the raw data.

#### LABORATORY TESTING

The SAMS system was assembled in a test area with two stable tables and light tunnel to offset vibration, light, and air scintillation effects. A laser interferometer, with an absolute accuracy of 6  $\mu$  inches (0.15 microns),

was installed as a measurement standard against which the position of the targets would be compared. Light emitting diode and retrodirective targets were mounted on an x-y, remotely operated, positioning device. Target positions were inserted into the system, verified by the interferometer, and sampled by the receiver/computer subsystem. Approximately 640 samples per measurement were used to establish the RMS accuracies. Target range was initially limited to 14 meters, the distance between the stable tables, which are isolated from the building structure; however, one and then two optical mirrors were used to increase ranges to 28 and 42 meters. Attempts of less than 14 meters range, by mounting the receiver on the floor between the stable tables, provided poor data. This was due to building vibrations transmitted through the floor. A summary of the laboratory test results is shown in Table 1. The accuracies are RMS of the raw data when compared to the laser interferometer standard.

TABLE 1

SURFACE ACCURACY MEASUREMENT SENSOR LABORATORY TESTS SUMMARY

<u>TARGET TYPE</u>	<u>RANGE</u>		<u>MM</u>	<u>INCHES</u>	<u>ACCURACY</u>
	<u>METERS</u>	<u>FEET</u>			<u>ARC SECONDS</u>
LED	14	46	±0.014	±0.000551	±0.206
LED	28	92	±0.100	±0.003937	±0.737
LED	42	138	±0.160	±0.006299	±0.786

50 METER ANTENNA SURFACE MODEL TEST

The SAMS system was transported to the Harris Corporation, Melbourne, Florida, and installed on a 50 Meter Antenna Surface Model. This model, see

figures 11 and 12, is a 30 degree, 4 gore, mesh segment of a 48 gore 50 meter diameter antenna.

The first portion of the test was devoted to a determination of the system stability in the test environment that might produce an effect from lights, vibration, scintillation, or RF interference. In order to provide the resolution and accuracy of the sensor, good data would depend on the stability of the structure during the test period. Consequently the structure holding the mesh model was instrumented with copper-constantan thermocouples and monitored to provide information on the stability of the antenna structure as a function of temperature. After monitoring structure temperatures for an extended period, it was determined that a 4-hour period of structure temperature stability was available for testing the sensor stability. Figures 13 and 14 show the relative stabilities of mesh LED-4 and hoop LED-5 targets during a typical 4-hour test. In these two figures, the approximately 0.100 inch (2.54 mm) displacement exhibited by LED-4 represents a vertical position change, effected by the manual adjustment of the mesh suspension system, for that point to check with the theodolite instruments system. Table 2 is a summary of the stability tests and indicates the RMS resolution of the sensor system.

TABLE 2

SURFACE ACCURACY MEASUREMENT SENSOR ANTENNA MODEL TEST RESULTS

FOR STABILITY TESTS

TARGET TYPE	RANGE		MM	RESOLUTION	
	METERS	FEET		INCHES	ARC SECONDS
LED 3	10.5	34.5	±0.015	±0.000591	±0.295
LED 4	15.7	51.5	±0.029	±0.001142	±0.381
LED 5	21.0	69.0	±0.060	±0.002362	±0.589

After determining that there were minimal effects from the test environment, displacement tests were conducted, using the theodolites as the standard of measurement. The Harris Corporation provided the calibrated theodolites, reported to have an accuracy of  $\pm 0.020$  inch (0.508 mm), and their computer aided operation. Using the theodolites for positioning, each mesh target was moved, by adjusting tension cords that were perpendicular to the surface, through a total displacement of 0.300 inch (7.620 mm) in ten steps. At each step, measurements were taken by both the theodolite system, which included 3 or 4 theodolites, and the SAMS system. Tables 3, 4, and 5 are tabulations of these results, along with the computed standard of deviation for each set of measurements.

## CONCLUDING REMARKS

The surface accuracy measurement sensor, through laboratory testing and by field tests on a mesh antenna model, has proven to be extremely accurate for displacement type measurements. That is, displacements that might result from thermal or dynamic distortions of a large space structure. Either LED or retrodirective reflector type targets can be used within existing antenna accuracy requirements. Except for single target viewing, the retro reflectors lack discrimination when more than one target is in the receivers field of view.

Recommendations for improvements that could be made to the sensors are as follows:

1. Lasers should be investigated as target light sources because they exhibit a much more concentrated beam, while using only one tenth the LED power.

2. Advanced photo diode detectors, with longer sensitive lengths, could provide a better linear response than that of the present detector.

Finally, it is felt that the breadboard system has good possibilities of being adapted to a flight system through miniaturization and that real time measurements could be quite useful to structures that require active shape control.

#### REFERENCES

1. Neiswander, Roberts.: Surface Accuracy Measurement Sensor for Deployable Reflector Antennas, NASA CR-154263, 1980.
2. Preliminary Design of an Engineering Model Surface Accuracy Measurement Sensor for Deployable Reflector Antennas. Final Technical Report, NASA Contract NAS1-16461, TRW Report 37714-6002-UT-00, dated September 30, 1981.

TABLE 3. LED-3 DISPLACEMENT TEST RESULTS

Target Nominal Position	SAMS Measurement	Theopolite Measurement (Standard)	Error (SAMS vs STD) E	Variance $(E - E_M) / V$	$v^2 \times 10^{-4}$
Inches	Inches	Inches	Inches	Inches	
+0.150	+0.1470	+0.1411	+0.0059	+0.0068	0.4624
+0.120	+0.1160	+0.1165	-0.0005	+0.0004	0.0016
+0.090	+0.0910	+0.0913	-0.0003	+0.0006	0.0036
+0.060	+0.0541	+0.0609	-0.0068	-0.0059	0.3481
+0.030	+0.0300	+0.0230	+0.0070	+0.0079	0.6241
0.000	-0.0098	0.0000	-0.0098	-0.0089	0.7921
-0.030	-0.0352	-0.0357	-0.0005	+0.0004	0.0016
-0.060	-0.0662	-0.0571	+0.0091	+0.0100	1.0000
-0.090	-0.0949	-0.0986	-0.0037	-0.0028	0.0784
-0.120	-0.1199	-0.1220	-0.0021	-0.0012	0.0144
-0.150	-0.1451	-0.1535	-0.0084	-0.0075	0.5625

$$\Sigma E = -0.0101$$

$$\Sigma v^2 = 3.8888 \times 10^{-4}$$

$$\text{Mean Error, } E_M = -0.0009$$

N = Number of measurements

$$\text{Standard of deviation} = \sqrt{\frac{\Sigma v^2}{N-1}} = 0.0062 \text{ Inch} \\ (0.1584 \text{ mm})$$



TABLE 4. LED-4 DISPLACEMENT TEST RESULTS

Target Nominal Position	SAMS Measurement	Theopolite Measurement (Standard)	Error (SAMS vs STD) E	Variance (E - E <sub>M</sub> ) V	V <sup>2</sup> × 10 <sup>-4</sup>
Inches	Inches	Inches	Inches	Inches	
+0.150	+0.1504	+0.1506	-0.0002	-0.0014	0.0196
+0.120	+0.1253	+0.1190	+0.0063	+0.0051	0.2601
+0.090	+0.0909	+0.0849	+0.0060	+0.0048	0.2304
+0.060	+0.0527	+0.0536	-0.0009	-0.0021	0.0441
+0.030	+0.0316	+0.0242	+0.0074	+0.0062	0.3844
0.000	-0.0031	0.0000	-0.0031	-0.0043	0.1849
-0.030	-0.0235	-0.0263	-0.0028	-0.0040	0.1600
-0.060	-0.0472	-0.0436	+0.0036	+0.0024	0.0576
-0.090	-0.0786	-0.0860	-0.0074	-0.0086	0.7396
-0.120	-0.1168	-0.1148	+0.0020	+0.0008	0.0064
-0.150	-0.1423	-0.1399	+0.0024	+0.0012	0.0144

$$\Sigma E = +0.0133$$

$$\Sigma V^2 = 2.1015 \times 10^{-4}$$

$$\text{Mean Error, } E_M = +0.0012$$

N = Number of measurements

$$\text{Standard of deviation} = \sqrt{\frac{\Sigma V^2}{N-1}} = 0.0046 \text{ Inch} \\ (0.1165 \text{ mm})$$

TABLE 5. RETRO REFLECTOR DISPLACEMENT TEST RESULTS

Target Nominal Position	SAMS Measurement	Theopolite Measurement (Standard)	Error (SAMS vs STD) E	Variance (E - E <sub>M</sub> ) V	v <sup>2</sup> × 10 <sup>-4</sup>
Inches	Inches	Inches	Inches	Inches	
+0.150	+0.1432	+0.1506	-0.0074	-0.0069	0.4761
+0.120	+0.1154	+0.1196	-0.0042	-0.0037	0.1369
+0.090	+0.0902	+0.0982	-0.0080	-0.0075	0.5625
+0.060	+0.0694	+0.0650	+0.0044	+0.0049	0.2401
+0.030	+0.0405	+0.0347	+0.0058	+0.0063	0.3969
0.000	+0.0155	0.0000	+0.0155	+0.0160	2.5600
-0.030	-0.0223	-0.0292	-0.0069	-0.0064	0.4096
-0.060	-0.0535	-0.0518	+0.0017	+0.0022	0.0484
-0.090	-0.0810	-0.0793	+0.0017	+0.0022	0.0484
-0.120	-0.1097	-0.1087	+0.0010	+0.0015	0.0225
-0.150	-0.1332	-0.1423	-0.0091	-0.0086	0.7396

$$\Sigma E = -0.0055$$

$$\Sigma V^2 = 5.6410 \times 10^{-4}$$

$$\text{Mean error, } E_M = -0.0005$$

N = Number of measurements

$$\text{Standard of deviation} = \sqrt{\frac{\Sigma V^2}{N-1}} = 0.0075 \text{ Inch} \\ (0.1915 \text{ mm})$$

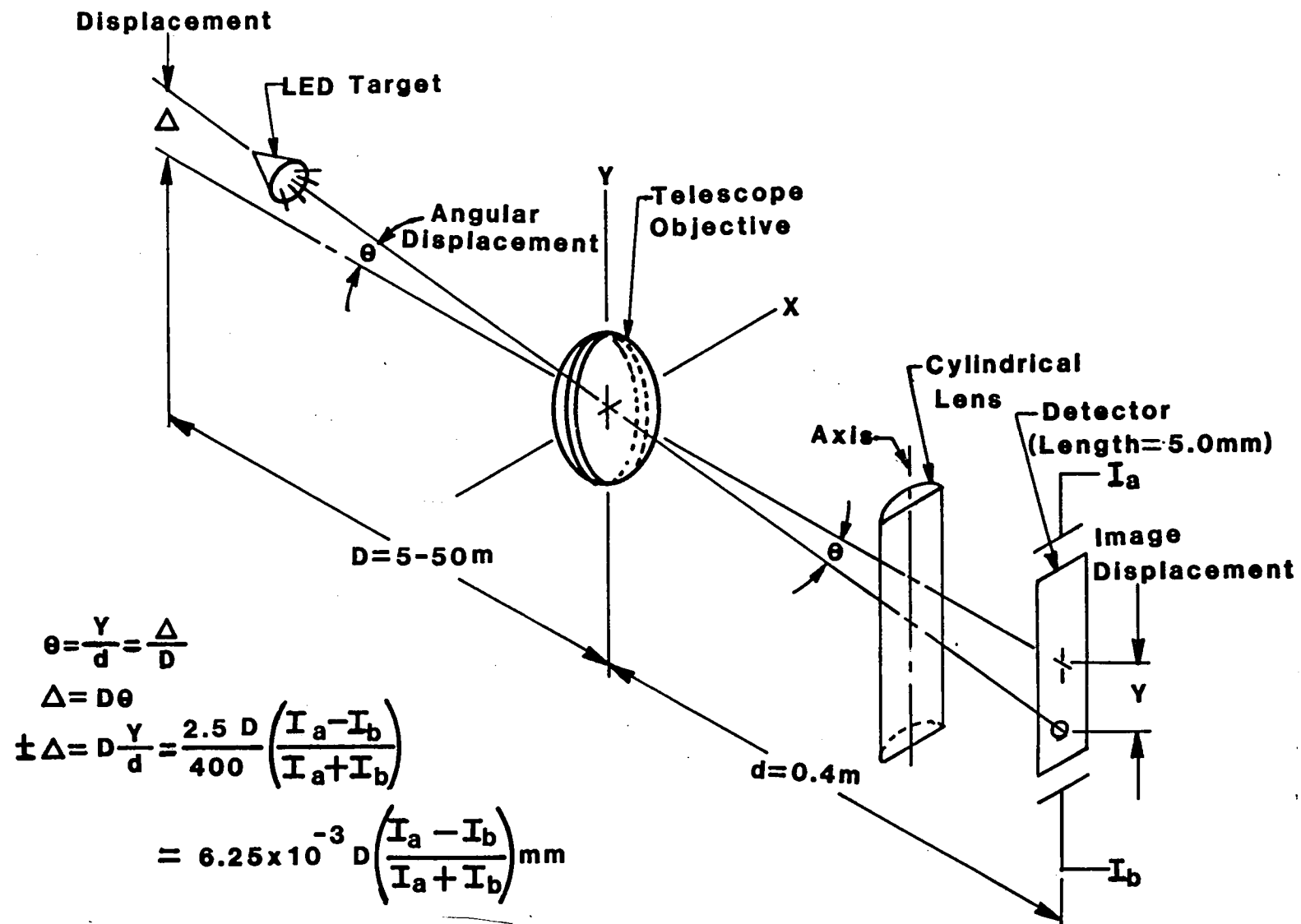


**Figure 1. Anamorphic Telescope Receiver With LED Target**

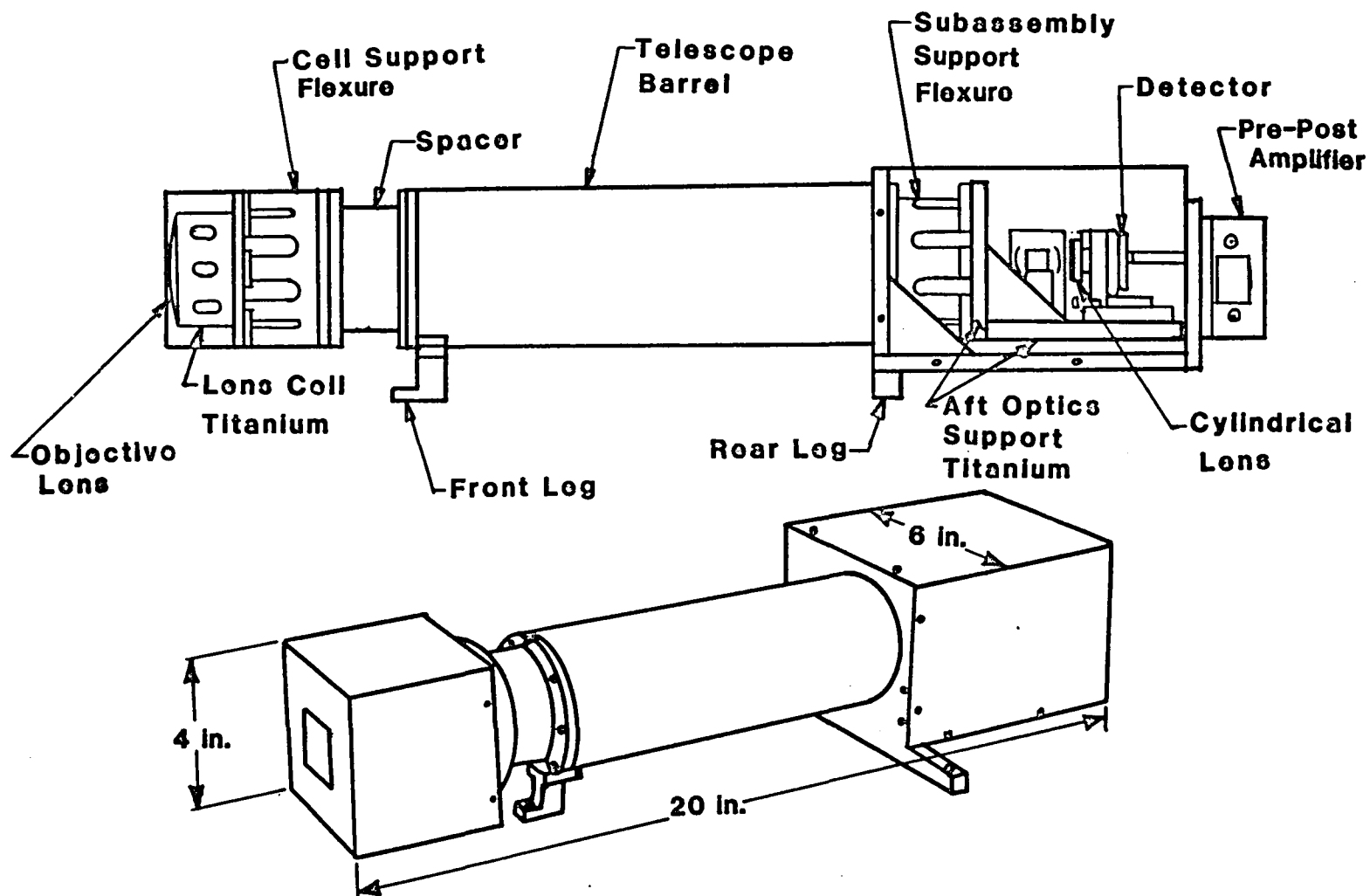


**Figure 2. SAMS Breadboard Receiver**

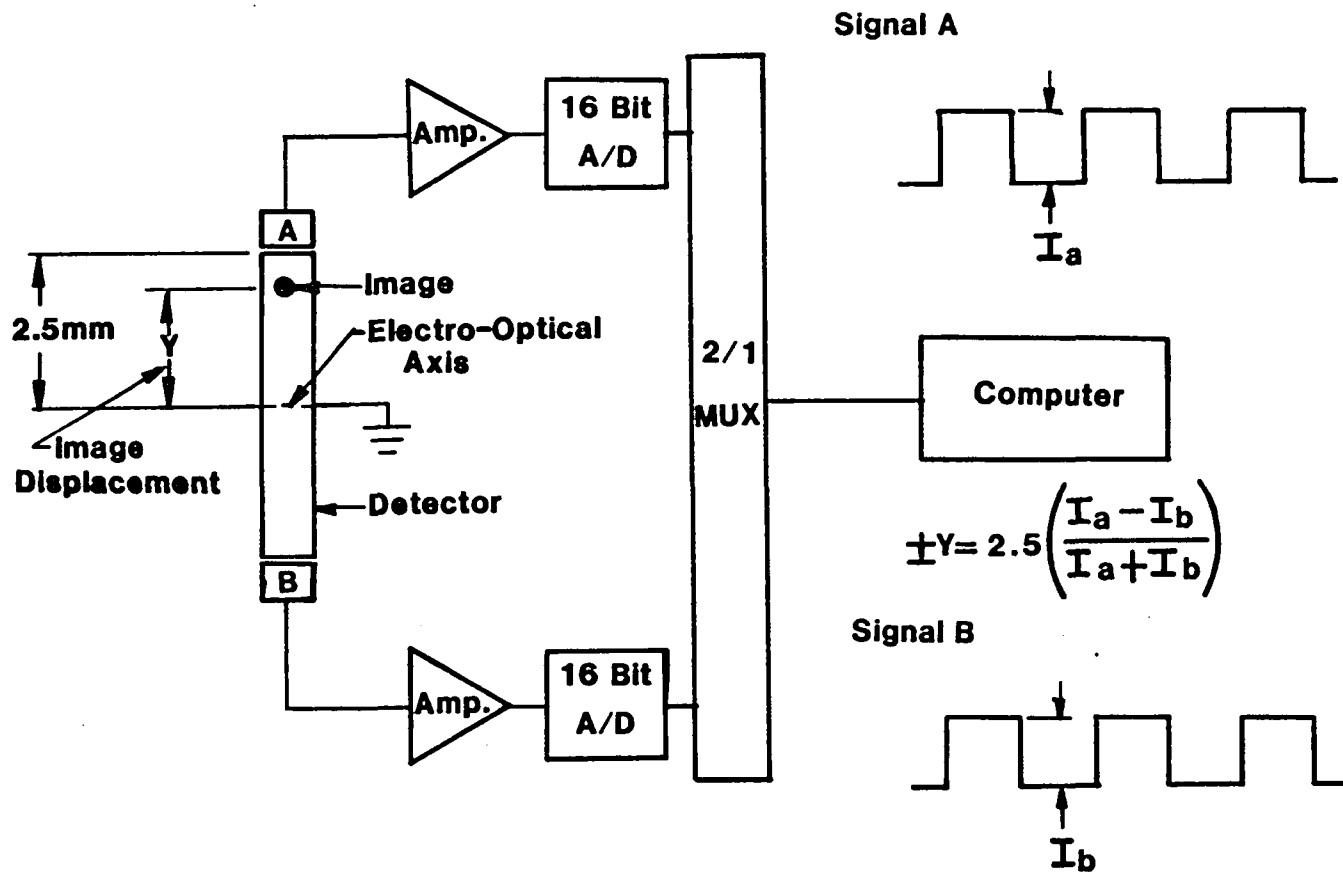


Figure 3. Receiver Detector Schematic

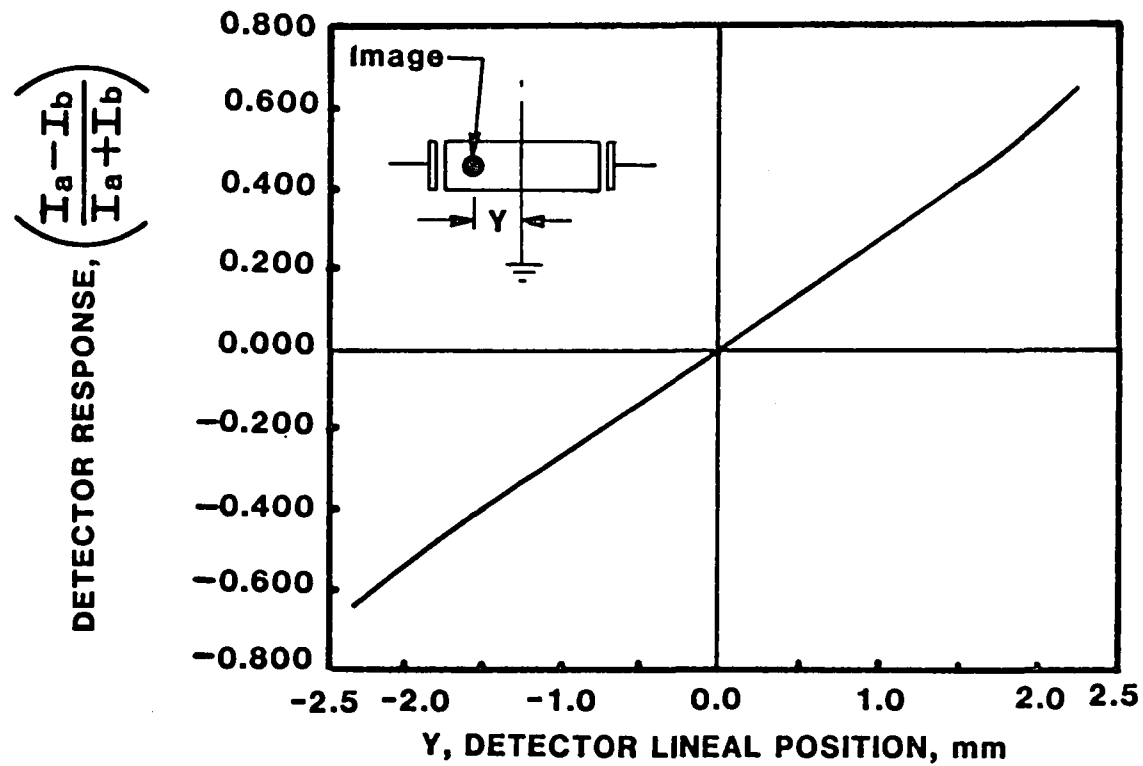


Figure 4. Single Axis Coordinate Detector Response

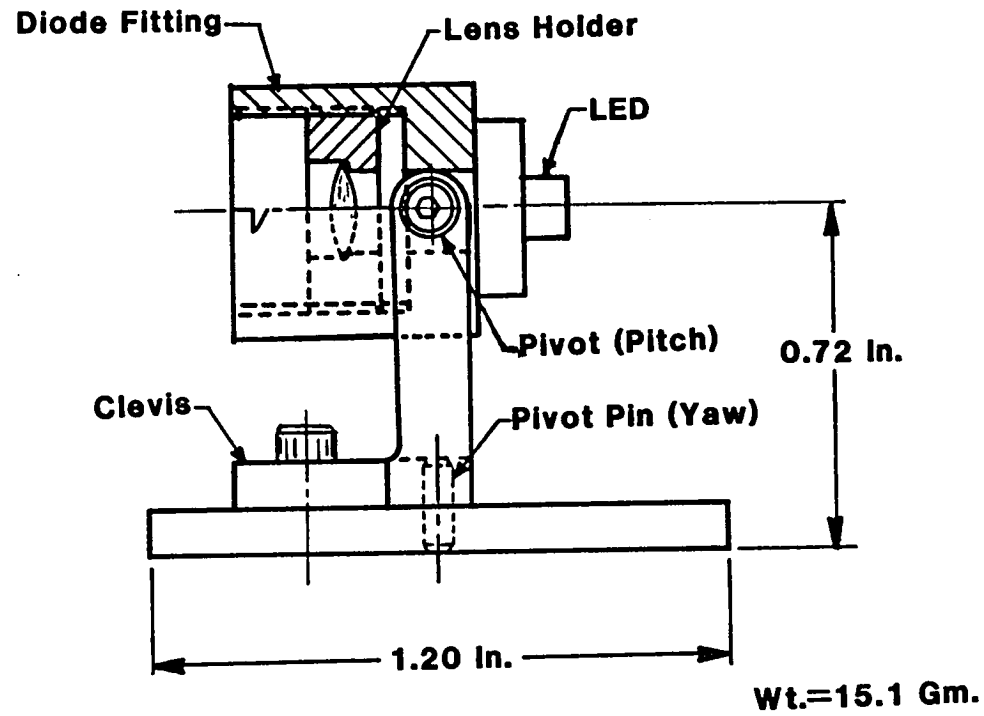
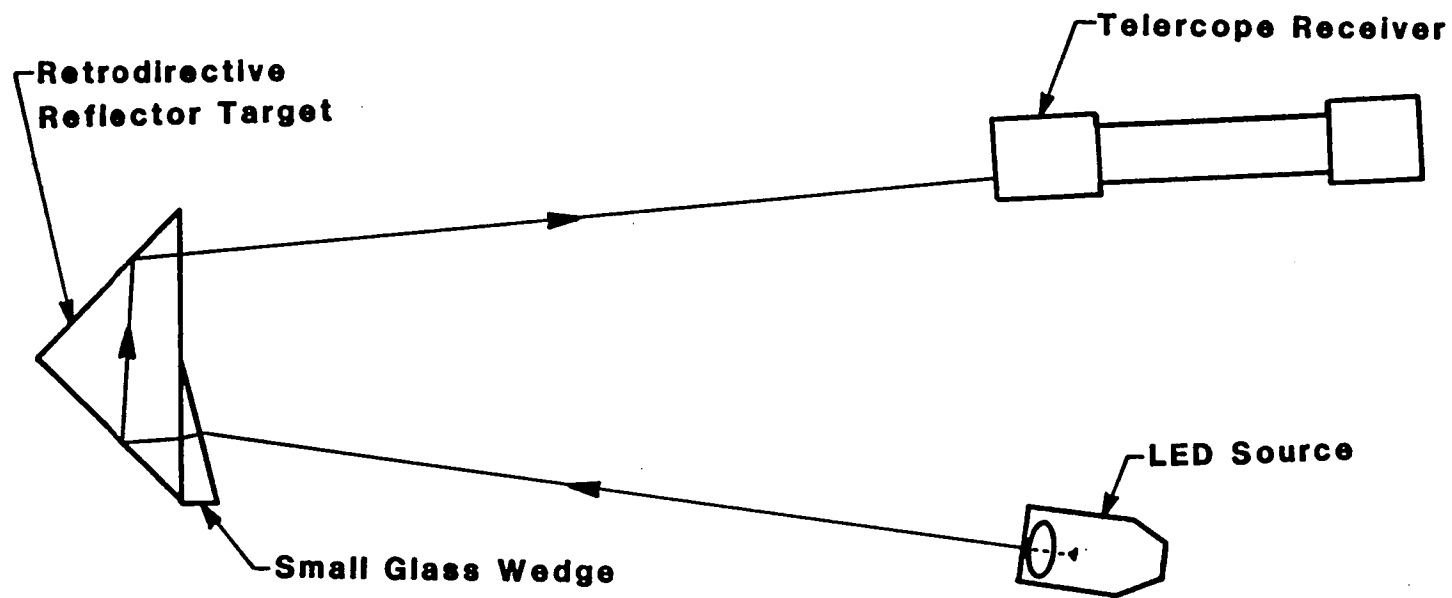


Figure 5. Light Emitting Diode Target

**Figure 6. Schematic, LED Driver, SAMS Breadboard**





**Figure 7. Passive Retrodirective Reflector Target**

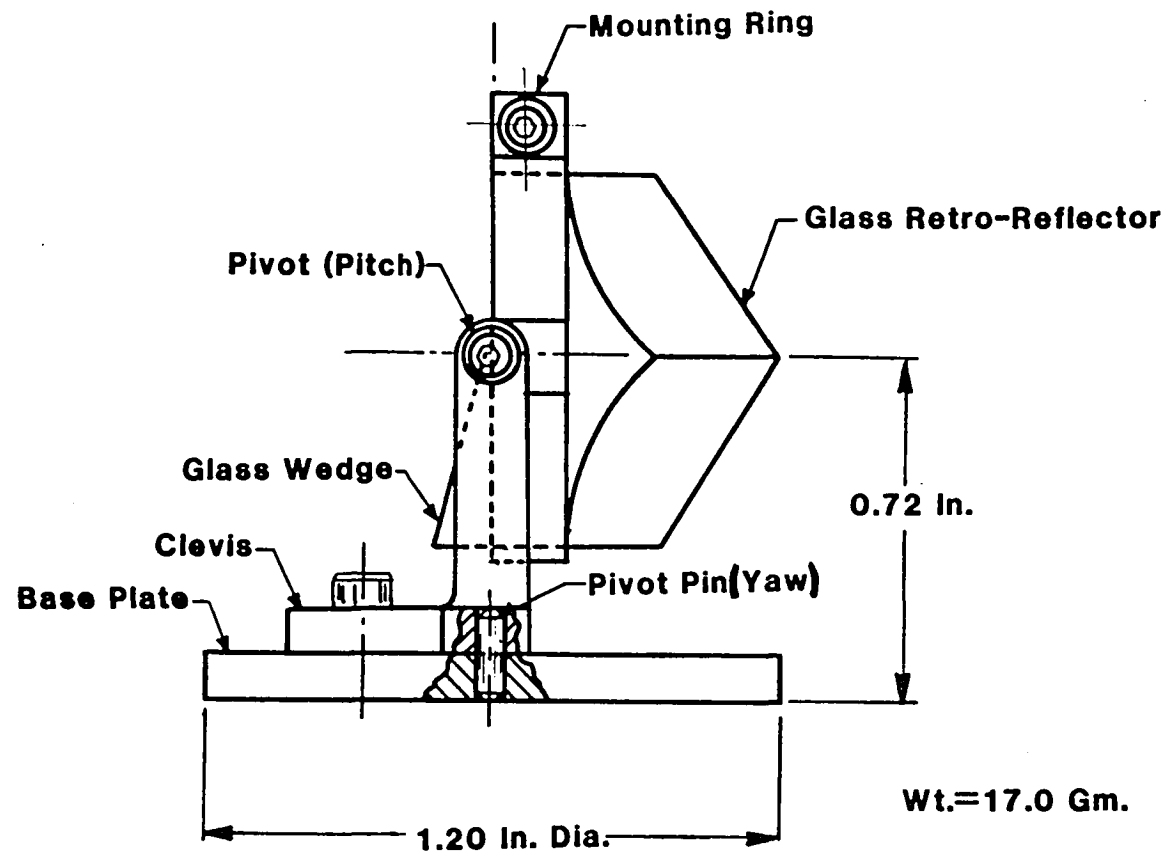


Figure 8. Retro-Reflector Target

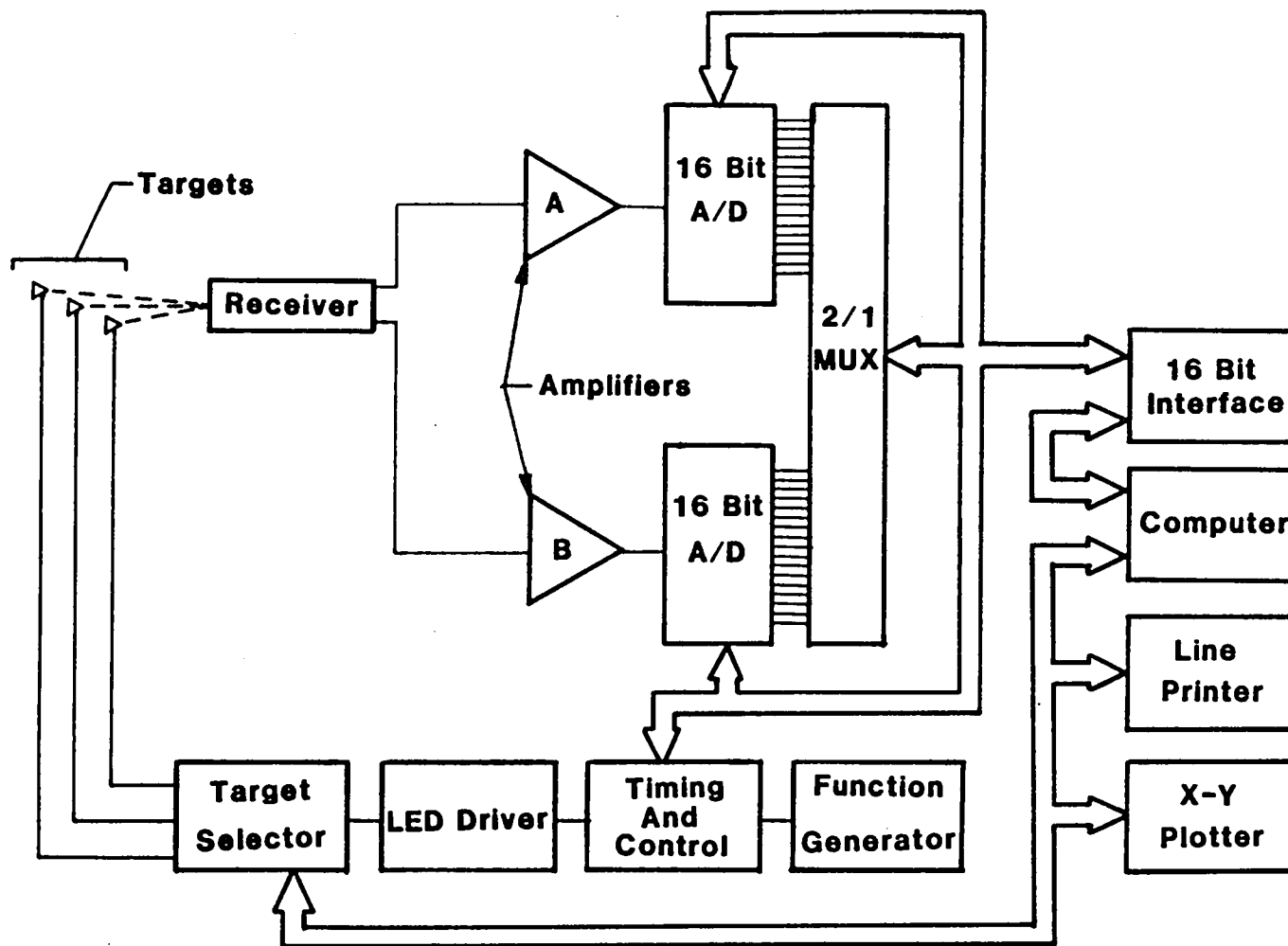
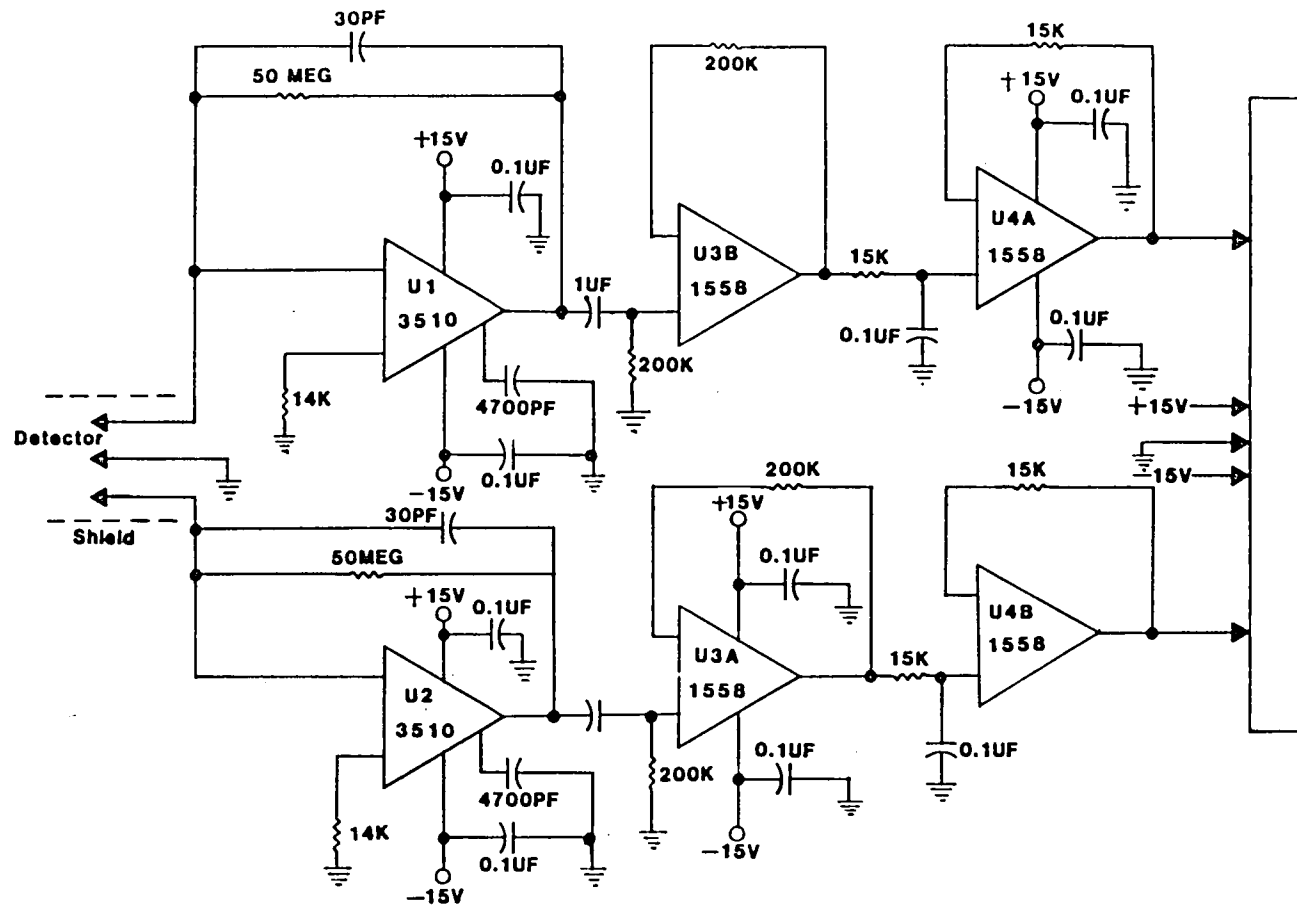
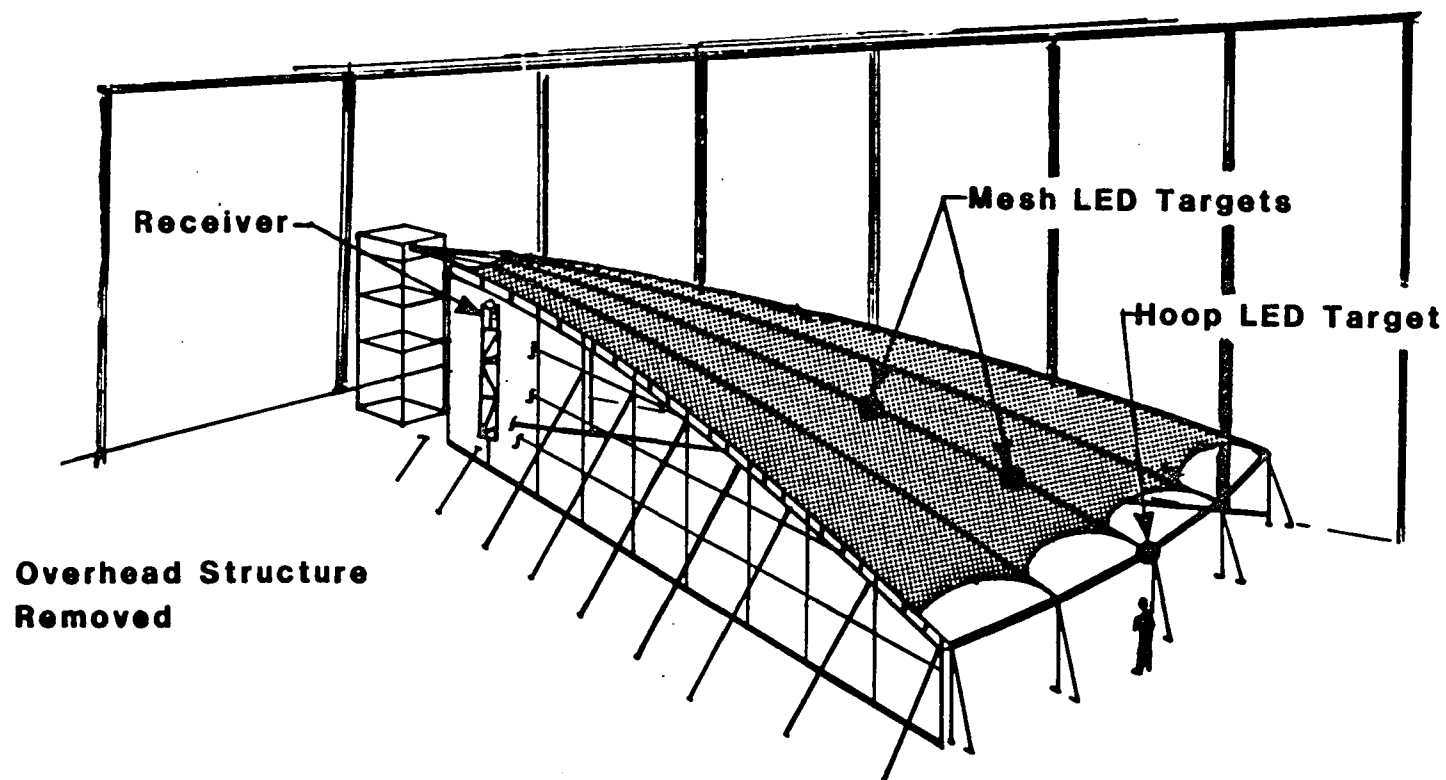


Figure 9. SAMS Electrical Schematic



**Figure 10. SAMS Breadboard Receiver Post-Preamplifiers**  
Schematic



**Figure 11. Surface Accuracy Measurement Sensor Test**  
**On 50 Meter Model**

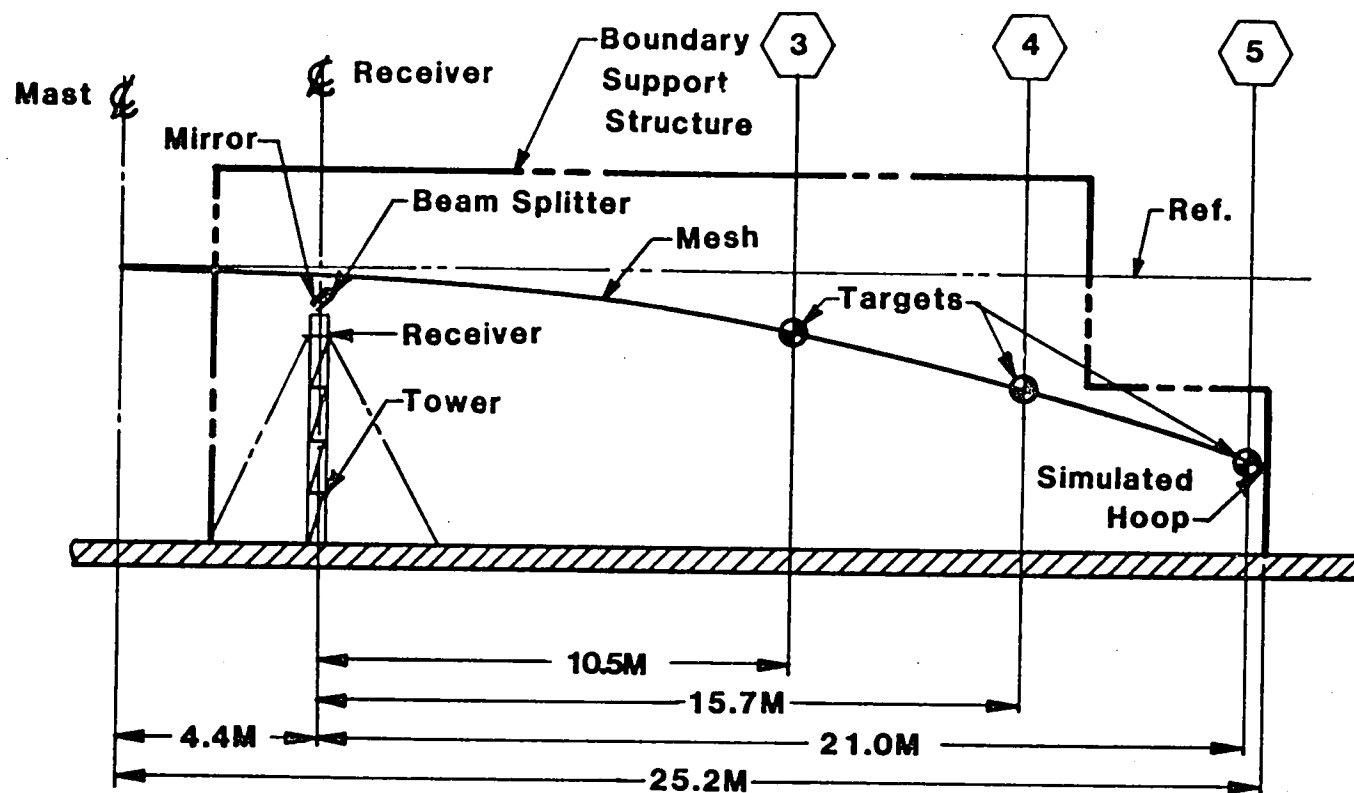


Figure 12. SAMS Antenna Model Test Arrangement

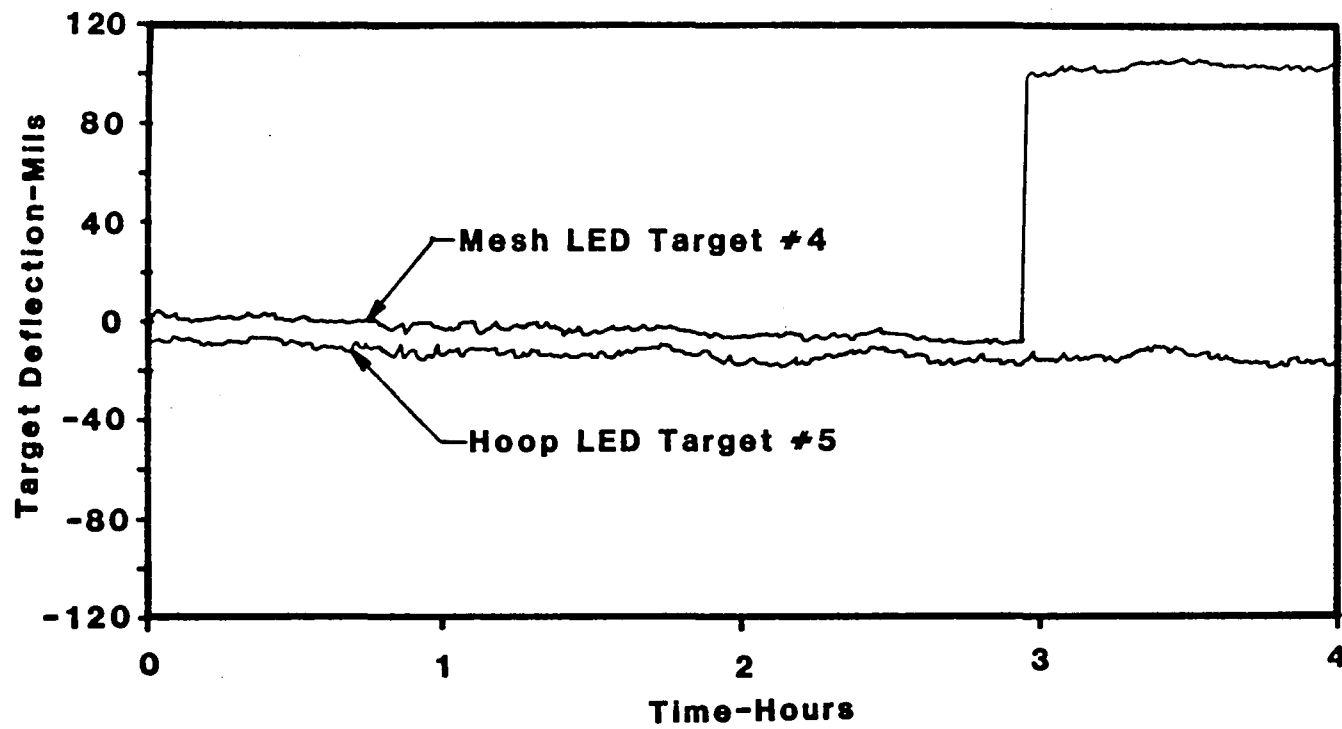


Figure 13. Stability And Displacement Test

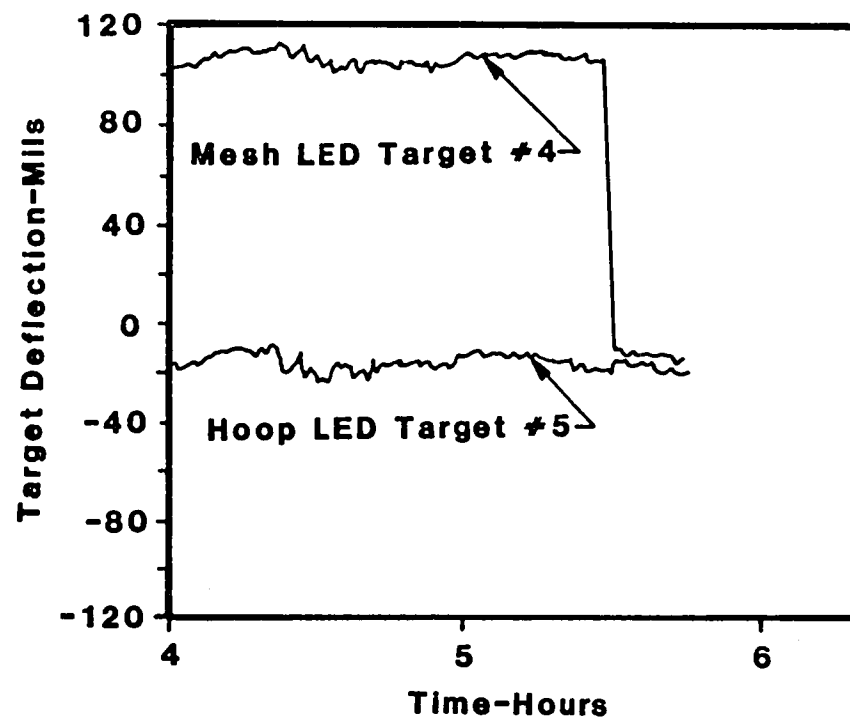


Figure 14. Stability And Displacement Test, (Cont.)





1. Report No. NASA TM-85689		2. Government Accession No.		3. Recipient's Catalog No.	
4. Title and Subtitle SURFACE ACCURACY MEASUREMENT SENSOR TEST ON A 50-METER ANTENNA SURFACE MODEL				5. Report Date January 1984	
				6. Performing Organization Code 506-53-43-12	
7. Author(s) *Robert B. Spiers, *Ernest E. Burcher, *Charles W. Stump, *Charles G. Saunders, and **G. F. Brooks				8. Performing Organization Report No.	
9. Performing Organization Name and Address  NASA Langley Research Center Hampton, VA 23665				10. Work Unit No.	
				11. Contract or Grant No.	
12. Sponsoring Agency Name and Address  National Aeronautics and Space Administration Washington, DC 20546				13. Type of Report and Period Covered Technical Memorandum	
				14. Sponsoring Agency Code	
15. Supplementary Notes  *NASA Langley Research Center **Kentron International, Inc.					
16. Abstract  The Surface Accuracy Measurement Sensor (SAMS) is a telescope with a focal plane photo electric detector that senses the lateral position of light source targets in its field of view. After extensive laboratory testing at NASA-Langley Research Center, the engineering breadboard sensor system was installed and tested on a 30 degree segment of a 50-meter diameter, mesh surface, antenna model. Test results correlated well with the laboratory tests and indicated accuracies of approximately 0.59 arc seconds at 21 meters range. Test results are presented and recommendations given for sensor improvements.					
17. Key Words (Suggested by Author(s))  Surface accuracy measurement sensor Large space antennas			18. Distribution Statement  Unclassified - Unlimited  Subject Category 32		
19. Security Classif. (of this report) Unclassified	20. Security Classif. (of this page) Unclassified	21. No. of Pages 31	22. Price A03		

5

7

5

•

4  
1  
1

4  
1  
1